Publications of the Astronomical Society of the Pacific
108: 615–619, 1996 July

The First Diffraction-Limited Images from the W. M. Keck Telescope

K. MATTHEWS

Palomar Observatory, California Institute of Technology, 320-47, Pasadena, California 91125
Electronic mail: kym@caltech.edu

A. M. GHEZ

Department of Physics and Astronomy, University of California, Los Angeles, California 90095
Electronic mail: ghez@astro.ucla.edu

A. J. WEINBERGER AND G. NEUGEBAUER

Palomar Observatory, California Institute of Technology, 320-47, Pasadena, California 91125
Electronic mail: alycia@mop.caltech.edu, gxn@caltech.edu

Received 1996 March 15; accepted 1996 May 1

ABSTRACT. The first diffraction limited, 0.″05 resolution, images on the W. M. Keck Telescope have been obtained at a wavelength of 2.2 μm. These images were part of an experiment to test the suitability of the Keck Telescope for speckle imaging. In order to conduct this test, it was necessary to modify the pixel scale of the Keck facility Near Infrared Camera (NIRC) to optimally sample the spatial frequencies made available by the Keck telescope. The design and implementation of the external reimaging optics, which convert the standard *f*/25 beam from the secondary mirror to *f*/182, are described here. Techniques for reducing speckle data with field rotation on an alt-az telescope are also described. Three binary stars were observed in this experiment with separations as small as 0.″05. With only 100 frames of data on each, a dynamic range of at least 3.5 mag was achieved in all cases. These observations imply that a companion as faint as 14.5 mag at 2.2 μm could be detected around an 11th magnitude point source.

1. INTRODUCTION

One potential advantage of large telescopes is the increase in the angular resolution of astronomical measurements. Traditionally, however, the angular resolution of ground-based telescopes has been limited not by the diffraction limit, but rather by index of refraction fluctuations in the Earth's atmosphere. At 2.2 μm, this resolution is typically 0.″5 at the W. M. Keck Telescope, a factor of 10 times worse than the theoretical limit.

Today there are several techniques, varying widely in complexity, which are capable of producing diffraction-limited observations from the ground. The "simplest" method, in terms of hardware, is speckle imaging. This technique compensates for the Earth's atmosphere in post-processing as opposed to adaptive optics, which corrects atmospheric phase perturbations in real-time. In recent years, two-dimensional near-infrared diffraction-limited images have been routinely made with speckle imaging at the Hale 200-inch Telescope at Palomar Observatory (Ghez et al. 1991, 1993; Koresko et al. 1993), the Steward Observatory 2.3-m Telescope (Henry et al. 1992, 1992; McCarthy et al. 1991, 1994), the 4-m at CTIO (Jura et al. 1995), the MMT (McLeod et al. 1991), and the ESO 3.5-m (Leinert et al. 1993).

The Keck Telescope, with a hexagonal primary mirror made up of 36 segments, has a maximum dimension across its face of 11 m (Nelson et al. 1985) and therefore offers the opportunity to obtain images which have an angular resolution a factor of 2–4 times higher than previous speckle imaging experiments. In this paper, we (1) describe the modifications which were made to the Keck facility near-infrared camera (NIRC) (Matthews and Soifer 1994) such that it can be used for speckle-imaging experiments and (2) present the first diffraction-limited images from Keck, with an angular resolution of 50 milliarcseconds.

2. DESIGN OF REIMAGING SYSTEM

In this section, we describe the NIRC Image Magnifier (IM), an ambient temperature assembly of optics which attaches to the NIRC dewar. The IM takes the *f*/25 beam from the secondary, which produces a scale of 0.15 arcsec pixel^{-1} on the detector, and converts it into an *f*/182 beam which produces a scale of 0.02 arcsec pixel^{-1} and a 5.″3 square field of view. This modified scale corresponds to Nyquist sampling for a wavelength of 2.2 μm, the center of the broad-band *K* filter, and a diameter of 11.0 m.

The design of the IM is shown in Fig. 1. It is an all reflecting, and therefore achromatic, approximately afocal system which magnifies the telescope image produced by the infrared secondary while maintaining the field and entrance pupil location as seen by NIRC. Specifically, the IM consists of five gold-coated mirrors: a convex and a concave spherical mirror (the 3rd and 4th optical elements in the light path, respectively), which create an off-axis Galilean telescope (see, e.g., Smith 1978), and three folding flats (1st, 2nd, and 5th elements) to feed the existing dewar optics and preserve

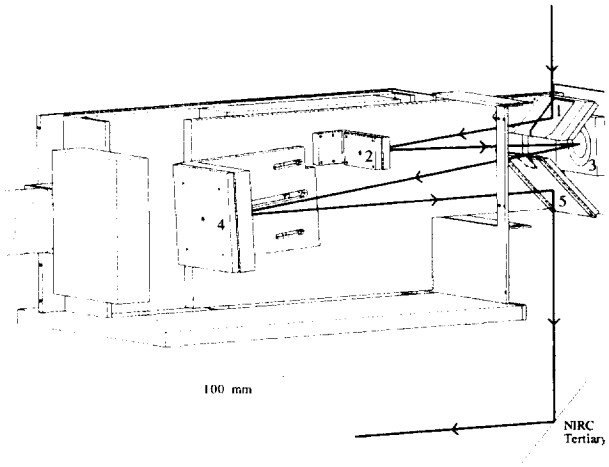

FIG. 1—Diagram of the Image Magnifier (IM) in its deployed position. A central ray is traced through the five mirrors, which are numbered according to their order, as described in the text. The light enters from the top of the drawing, and exits at the bottom. The fold mirror, shown at the bottom right, is mounted onto NIRC and is the tertiary mirror under direct-imaging conditions; when the IM stage is deployed, it instead takes light from the IM into NIRC.

the location of the focus. The optics were designed such that the chief ray lies in a plane; the image produced through the IM is therefore reflected about a line through the center of the array and parallel to the rows compared to a direct image. The last flat has a small segment of a circle removed to avoid occulting the beam. This introduces a negligible amount of vignetting (0.2% of the field of view). However this also allows a corresponding portion of the unmagnified field to bypass the IM. This is only an issue in a crowded field and generally has no effect on the observations. In a crowded field this portion (12.4%) is masked off in post-processing.

In order to make the IM a permanent addition to NIRC it was designed (1) to be easily deployed and retracted such that an observer can quickly switch between direct-imaging and speckle-imaging modes and (2) to contribute negligible excess thermal emission to the normal direct-imaging mode of operation. This was accomplished by mounting the IM optical bench on a stepper-motor-driven translation stage which itself was mounted directly onto NIRC. When the IM is deployed, the large flat pick-off mirror extends over the tertiary mirror assembly of NIRC and sends the beam through the IM. When the IM is retracted the optical bench completely clears the *f*/25 field by a sufficient margin to preclude contamination by excess thermal radiation. In its retracted position the IM is in a closed housing, which protects the optical elements from dust. The overall dimensions of the IM in its closed position are $0.19 \times 0.24 \times 0.46$ meters, where the first dimension is the height above NIRC. It takes about five seconds to deploy or retract the IM, thus allowing rapid switching between direct imaging and speckle modes.

3. OBSERVATIONS

The IM was tested during the night of 1995 April 18 (UT). The primary goal of the observations was to demonstrate that speckle imaging works on the segmented Keck Telescope. For these tests, four well-known close binary stars from Worley and Heinz (1983) and Ghez et al.(1995) were observed. Of these, results from three are reported in Table 1; one star was excluded from analysis because its calibrator was resolved.

Observations were made in sets of ten integrations on the source and one on the sky. A total of about ten sets, or ~100 frames, were collected on the object before the telescope was moved to a calibrator star (an unresolved point source) for another 100 frames. Although the individual integration times were 0.068 s or 0.10 s, the software configuration of NIRC at that time allowed only one exposure every 10 s, independent of the actual integration time.

As a result of the telescope's alt-az mounting, the relative orientation of the pupil to the sky changed with time. Since speckle-imaging analysis requires a constant telescope transfer function for the object and calibrator, the pupil's orienta-

TABLE 1
Journal of Observations

Object		ω Leo SAO 117717	β LMi SAO 62053	SR 20 HBC 643
K_{obj}	mag	4.1[a]	2.5[a]	7.1[b]
Spectral type		F9[c]	G9[c]	G0[d]
Calibrator		SAO 98627	SAO 62019	SAO 184429
K_{cal}	mag	3.1[a]	3.5[a]	5.4[a]
t_{exp}	s	0.1	0.068	0.068
λ	μm	2.21	2.16	2.21
Δλ	μm	0.43	0.02	0.43
Seeing	arcsec	0.9	1.1	0.8
Separation[e]	arcsec	0.517±0.006	0.062±0.004	0.040±0.002
Posn. angle	deg	71.0±0.7	317±8	145±6
Flux ratio		4±1	9.2±0.7	7±1

Notes to TABLE 1

[a] *K* magnitude was estimated based on V magnitude and stellar type.
[b] *K* magnitude from Simon et al. (1995).
[c] Spectral type from SAO catalog.
[d] Spectral type from Bouvier and Appenzeller (1991)
[e] Quoted uncertainties do not include uncertainties in pixel scale of the detector.

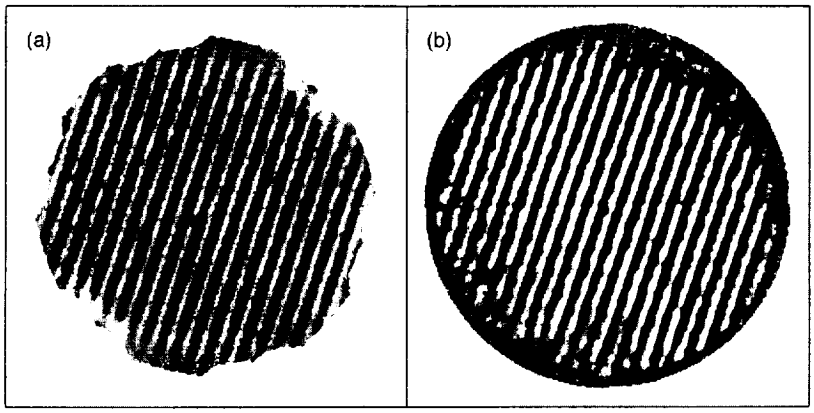

FIG. 2—Computed estimates of the real and imaginary parts of the Fourier transform of the binary star ω Leo (SAO 117717): (a) power spectrum ($|O(\mathbf{u})|^2$ from Eq. 1) and (b) phases. Note that in (a) the fringes extend to the edges of the pupil. The shape of the pupil results from the hexagonal primary (less two of its mirrors) rotating through 23° during the observations.

tion was kept fixed with respect to the IM and NIRC and the field allowed to rotate on the detector throughout the observations. This was done by keeping the telescope's instrument rotator immobile during each complete set of observations on an object and its associated calibrator.

Throughout the observations there was a partial malfunction of the telescope's active control system. The consequence of this was the loss of 2 of the 36 segments from the image stack and a degradation of the rms phasing from the ~ 100 nm achieved seven days prior to this run to about 1 μm. During these observations the image size varied between 0".8 and 1".2 FWHM at 2.2 μm.

4. DATA ANALYSIS

In preliminary processing, each image was sky subtracted and flat fielded, and bad pixels were corrected by interpolation. In the second stage of analysis, the object's Fourier amplitudes and phases were recovered via classical speckle analysis (Labeyrie 1970) and bispectral analysis (Weigelt et al. 1987; Gorham et al. 1989), respectively. In both processes, the standard procedure was modified as described below to incorporate the field rotation that occurred during the observations. No part of this method requires a model of the source structure.

The sky and calibrator brightness distributions as well as the atmospheric transfer function were assumed to be independent of orientation on the sky. This allowed the ensemble averages of their power spectra to be calculated without accounting for field rotation. The power due to array noise, estimated by the ensemble sky power spectrum, was subtracted from each object power spectrum and the average calibrator power spectrum. Finally, each object power spectrum was calibrated and rotated to a fixed orientation with respect to the sky. The results were averaged together to produce an estimate of the object's power spectrum.

The process described above can be expressed as

$$|O(\mathbf{u})|^2 = \frac{1}{N}\sum_{i=1}^{N} \mathcal{R}_i \frac{|I_i(\mathbf{u}')|^2 - \langle|S(\mathbf{u}')|^2\rangle}{\langle|C(\mathbf{u}')|^2\rangle - \langle|S(\mathbf{u}')|^2\rangle}. \quad (1)$$

In this equation, $|I_i(\mathbf{u}')|^2$, $\langle|S(\mathbf{u}')|^2\rangle$, and $\langle|C(\mathbf{u}')|^2\rangle$ are the individual object frame power spectrum, ensemble averaged sky power spectra, and ensemble averaged calibrator power spectra, respectively, where $\mathbf{u}' = (u', v')$ is the spatial frequency on the sky. $|O(\mathbf{u})|^2$ is the estimate of the object's power spectrum where $\mathbf{u}$ is the spatial frequency in the rotated Fourier space. $\mathcal{R}$ denotes the rotation matrix from pupil to sky coordinates, i denotes each individual object frame and N is the total number of object frames.

Due to the azimuthal asymmetry of the Keck mirror and its alt-az mount, the Fourier transform of the pupil is asymmetric and rotates over time; therefore, the $u-v$ coverage of the source also rotates over time. In order to keep only high signal-to-noise ratio points, only data at spatial frequencies for which the pupil transform was non-zero in every exposure were included in the averages. The power at all other spatial frequencies was set to zero.

For the Fourier phase analysis, the Fourier transform of each image frame was similarly rotated before computing the bispectrum. The total number of unique possible points in the four-dimensional bispectrum for this system, out to a maximum spatial frequency corresponding to the full 11-m mirror, was over 110 million, which exceeded the ~30,000 unknown phases. Thus the phase solution was greatly overconstrained. To make the computation more tractable, only phases out to a maximum spatial frequency corresponding to a 10-m mirror (22 cycles arcsec^{-1}) and the "near-axis" ($|u|$ or $|v| \leq 0.4$ cycles arcsec^{-1}) portion of the bispectrum were considered. This reduced the number of bispectral points to 294,747 (Gorham et al. 1989).

As a final step, the Fourier amplitudes were multiplied by the transfer function of the telescope which was approximated by a Gaussian with a FWHM of 0".05. The resulting tapered amplitudes were combined with the phases and inverse Fourier transformed to produce a final image.

5. RESULTS

Binary stars have the distinctive visibility signature of a cosine whose frequency is proportional to their separation and whose amplitude of variation depends on their flux ratio. Figures 2 and 3 show the results from ω Leonis (SAO

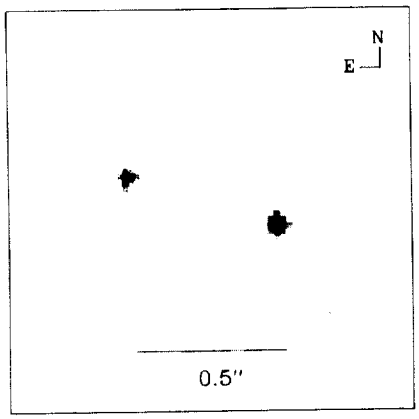

FIG. 3—Reconstructed diffraction-limited image of ω Leo. The resolution of this image is 0.″05.

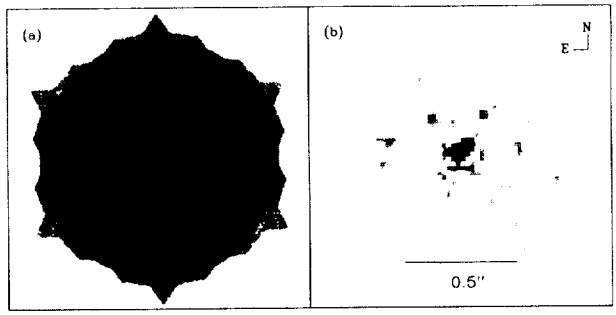

FIG. 4—(a) The power spectrum ($|O(\mathbf{u})|^2$ from Eq. 1) of the binary star β LMi (SAO 62053), which has a somewhat mottled appearance due to small miscalibrations of the individual segments. With only 100 exposures, this effect limited the dynamic range to 3.5 mag. (b) The final diffraction-limited image of β LMi showing the binary with a separation of 0.″06 and flux ratio of 2.4 mag.

117717). The fringe pattern in the spatial frequency domain of this binary-star system extends out to the highest expected spatial frequencies in most directions. A slight loss in power is detectable in the upper right and lower left; this is a consequence of the two misaligned mirror segments. The irregularities from the fringe pattern in the central region, the lowest spatial frequencies, of the power spectrum (Fig. 2a) are probably the result of variation in the seeing between the time the object and calibrator were observed (Christou 1985).

The measured properties for the binary stars observed, which are listed in Table 1, were obtained by fitting the known functional form for a binary star to the observed object power spectrum (see Ghez et al. 1995) and assuming that the IM pixel scale is the designed 0.0206 arcsec pixel^{-1}. In addition, the result for ω Leo may be used in conjunction with measurements of the same source from Palomar and Steward Observatories (Ghez et al. 1995) to estimate the actual pixel scale of the NIRC plus IM system. A fit to the other measurements predicts a separation for ω Leo of 0.510 $\pm$0.010 arcsec at the time of the Keck observations. This corresponds to a detector scale of 0.0203 $\pm$ 0.0005 arcsec pixel^{-1} which is consistent with the design scale.

In general, the dynamic range of speckle observations is limited by noise in the power spectrum which originates from detector read noise and changes in the atmosphere and telescope between the observation of the object and of its calibrator. For the measurements reported in this paper, small changes in the relative phases of adjacent primary mirror segments between the observation of the object and of its calibrator produce the dominant source of noise. This effect, seen as a mottled pattern similar to that predicted from the segment spacing and wavelength of observation, can be seen particularly well in the divided power spectrum of β LMi (SAO 62053) (Fig. 4a). Nonetheless, a 1 σ dynamic range of at least 3.5 mag was achieved with only 100 exposures for each of the objects observed. This dynamic range could be increased by obtaining more frames of data and by observing at a variety of different pupil orientations to average out the segment effects.

Similarly, the limiting magnitude is a function of the seeing and the read noise of the detector. For these observations, we estimate a limiting magnitude of $K \approx 11$ mag by requiring that the SNR for the brightest speckle be greater than one; this limit should be a steep function of the seeing, so under better conditions one should be able to observe fainter objects. If a dynamic range of 3.5 mag can be achieved at this limit, companions separated by the diffraction limit and as faint as 14.5 mag would be detectable with speckle imaging.

6. CONCLUSIONS

The addition of the image magnifier to NIRC allows rapid switching between the standard direct-imaging pixel scale (0.15 arcsec pixel^{-1}) and a new one (0.02 arcsec pixel^{-1}) which provides Nyquist sampling for diffraction-limited imaging.

In the first use of speckle imaging on the 10-m Keck Telescope, three known binary-star systems with separations ranging from 0.″05 to 0.″5 were successfully imaged with diffraction-limited resolution. The dynamic range of these images, constructed with only 100, 0.1 s exposures, is 3.5 mag. Based on the signal-to-noise ratio of these observations, we estimate that the limiting magnitude for speckle imaging of point sources is $K=11$ mag, which, when combined with this dynamic range, means that companions as faint as 14.5 mag could be observed.

It is a pleasure to thank the W. M. Keck Foundation and its President, Howard B. Keck, for the generous grant that made the W. M. Keck Observatory possible. We thank the Keck Science Steering Committee for providing funds to construct the NIRC image magnifier, Jerry Nelson, Gary Chanon, and Michael DiVittorio for their work on the Keck optics, Barbara Schaefer and Terry Stickel, the telescope operators during these observations, and Wendy Harrison for assistance with the observations. We also thank Jonathan Kawamura and Sean Lin for their work on designing the image magnifier, Al Conrad for modifying NIRC software to facilitate speckle imaging at Keck, and Beth Klein for helping with the observations. Infrared astronomy at Caltech is supported by grants from the NSF. A. J. W. is supported through the NASA Graduate Student Researchers Program. A. M. G. is supported by a NSF Young Investigator Award.

REFERENCES

Bouvier, J., and Appenzeller, I. 1991, A&ASS, 92, 481
Christou, J. C., Cheng, A. Y. S., Hege, E. K., and Roddier, C. 1985, AJ, 90, 2644
Ghez, A. M., Neugebauer, G., Gorham, P. W., Haniff, C. A., Kulkarni, S. R., Matthews, K., Koresko, C., and Beckwith, S. 1991, AJ, 102, 2066
Ghez, A. M., Neugebauer, G., and Matthews, K. 1993, AJ, 106, 2005
Ghez, A. M., Weinberger, A. J., Neugebauer, G., Matthews, K., and McCarthy, D. W. 1995, AJ, 110, 753
Gorham, P. W., Ghez, A. M., Kulkarni, S. R., Nakajima, T., Neugebauer, G., Oke, J. B., and Prince, T. A. 1989, AJ, 98, 1783
Henry, T. J., McCarthy, D. W., Freeman, J., and Christou, J. C. 1992, AJ, 103, 1369
Jura, M., Ghez, A. M., White, R. J., McCarthy, D. W., Smith, R. C., and Martin, P. G. 1995, ApJ, 445, 451
Koresko, C. D., Beckwith, S., Ghez, A. M., Matthews, K., Herbst, T. M., and Smith, D. A. 1993, AJ, 105, 1481
Labeyrie, A. 1970, A&A, 6, 85
Leinert, Ch., Haas, M., and Weitzel, N. 1993, A&A, 271, 535
Matthews, K., and Soifer, B. T. 1994, Astronomy with Infrared Arrays: The Next Generation, ed. I. McLean (Dordrecht, Kluwer); Ap&SS, 190, 239
McCarthy, D. W., Henry, T. J., McLeod, B., and Christou, J. C. 1991, AJ, 101, 214
McCarthy, D. W., Freeman, J. D., and Drummond, J. D. 1994, Icarus, 108, 285
McLeod, B. A., McCarthy, D. W., and Freeman, J. D. 1991, AJ, 102, 1485
Nelson, J. E., Mast, T. S., and Faber, S. M. (ed.) 1985, The Design of the Keck Observatory and Telescope (Ten Meter Telescope), Keck Observatory Report No. 90
Simon, M., et al. 1995, ApJ, 443, 625
Smith, W. J. 1978, Handbook of Optics, ed. W. G. Driscoll (New York, McGraw-Hill), p. 2
Weigelt, G. 1987, Opt. Comm., 21, 55
Worley, C. E., and Heintz, W. D. 1983, PUSNO, 24, part 7